HHS Public Access

Author manuscript

Part Part Syst Charact. Author manuscript; available in PMC 2023 April 01.

Published in final edited form as:

Part Part Syst Charact. 2022 April ; 39(4): . doi:10.1002/ppsc.202100280.

Accelerating Cell Migration along Radially Aligned Nanofibers through the Addition of Electrosprayed Nanoparticles in a Radial Density Gradient

Jiajia Xue[†], **Tong Wu**[†], **Jichuan Qiu**[†], **Younan Xia**[†,‡,*]

[†]The Wallace H. Coulter Department of Biomedical Engineering, Georgia Institute of Technology and Emory University, Atlanta, Georgia 30332, United States

[‡]School of Chemistry and Biochemistry, School of Chemical and Biomolecular Engineering, Georgia Institute of Technology, Atlanta, Georgia 30332, United States

Abstract

Scaffolds capable of promoting cell migration from the periphery towards the center along the radial direction hold promises for tissue regeneration. Here we report a simple and general method based on masked electrospray for the fabrication of such scaffolds by depositing collagen nanoparticles on radially-aligned nanofibers in a radial density gradient. Placed between the metallic needle and the collector, an aperture with tunable opening sizes serves as the mask. By increasing the size of the opening at a fixed speed, the electrosprayed particles take a radial density gradient that decreases from the center to the periphery. When deposited on a glass slide, the radial density gradient of collagen nanoparticles promotes the migration of fibroblasts from the periphery towards the center. By replacing the glass slide with a scaffold comprised of radially-aligned nanofibers, a synergetic effect arises to further accelerate cell migration along the radial direction. The synergistic effect can be attributed to a unique combination of the topographic cue arising from the aligned nanofibers and the haptotactic cue enabled by the graded nanoparticles. This work demonstrates a method to maximize cell migration from the periphery towards the center through a combination of topographic and haptotactic cues.

Graphical Abstract

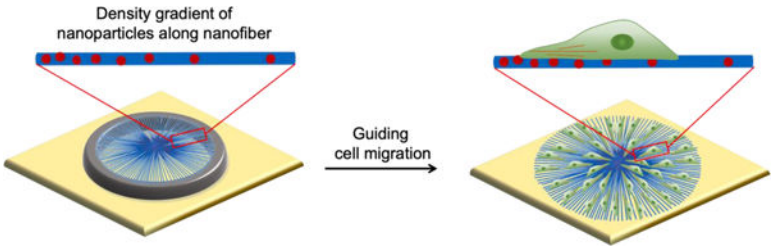

Two is better than one: Collagen nanoparticles are fabricated in a radial density gradient by masked electrospray with a tunable aperture. When deposited on a scaffold of radially-aligned

[*]Address correspondence to Y.X. (younan.xia@bme.gatech.edu).

Supporting Information

Supporting Information is available from the Wiley Online Library or from the author.

nanofibers, cell migration is accelerated due to the synergy between the topographic cue arising from the aligned nanofibers and the haptotactic cue enabled by the gradient of nanoparticles.

Keywords

Radially-aligned nanofibers; electrosprayed nanoparticles; radial density gradient; cell migration

1. Introduction

Cell migration plays an important role in many biological processes such as the regeneration of injured tissues.[1–3] Recruiting repairable cells from the surrounding healthy tissues to the injured site is one of the key requirements for tissue regeneration.[4–7] Specifically, the migration of cells from the periphery towards the center is required for the regeneration of many types of tissues.[8,9] For example, skin regeneration can be augmented by directing the migration of fibroblasts to the wound site for the re-establishment of dermis,[10] and the regeneration of dura mater requires the migration of cells from the periphery towards the center to cover the defected dura.[11] As another example, newborn cortical neurons in the developing cortex migrate along radial glial fibers towards the cortical plate to form the layered structure.[8,12] In addition, enhanced recruitment of endogenous neural stem cells from the central canal region to the lesion site is necessary for the repair of spinal cord injury to re-establish neural connectivity.[13] As such, it is of great importance to promote tissue regeneration by developing a scaffold capable of effectively guiding the radial migration of cells and directing their organization for the formation of functional tissue.

Cell migration can be directed by different means, such as topographic and haptotactic cues.[8,14,15] When designing a scaffold, these beneficial cues should be integrated to maximize their impact on cell migration. Despite major progress, it remains a major challenge to develop scaffolds that recapitulate the complex structure and microenvironment of native tissues. Among various types of scaffolding materials, electrospun fibers show great promises owing to their capability to mimic some structural and compositional features of the extracellular matrix (ECM) and the feasibility to combine both topographic and haptotactic cues in the same scaffold.[16–19] As reported in the literature, scaffolds comprised of radially-aligned nanofibers could provide a topographic cue to guide and accelerate cell migration along the radial direction, promoting wound closure.[11] Three-dimensional (3-D) scaffolds consisting of radially-aligned nanofibers could also promote diabetic wound healing.[10] Furthermore, radially-aligned nanofibers could direct the growth of retinal ganglion cell axons radially, mimicking the radial axon paths in the retina.[20,21]

In addition to the topographic cue, gradients represent another important type of cue in regulating the migration and assembly of cells.[1,22] A variety of strategies have been developed for incorporating radial gradients into the surface of a solid substrate.[23,25] For example, surface engineering through asymmetric chemical modification or geometrical patterning has been applied to generate graded features on a solid substrate such as silicon wafer or glass slide.[26,27] These methods usually require further modification steps with

the use of specific types of material precursors or the application of an elastomeric stamp. Selective deposition represents another strategy for generating radial gradients. Specifically, when integrated with radial gradients of bioactive components, scaffolds made of radially-aligned nanofibers can further accelerate the migration of cells from the periphery towards the center. In a previous study, we generated a radial gradient of active protein on a scaffold made of radially-aligned nanofibers by back-filling the bare regions left behind by a graded mask of bovine serum albumin with the active protein.[28] The radial gradient of laminin promoted the migration of fibroblasts while that of the epidermal growth factor worked for keratinocytes migration. Although this method can minimize the use of expensive growth factors, only a monolayer of the protein can be absorbed on the surface of the fibers.

As an electrohydrodynamic process, electrospray has been extensively explored to deposit particles on a solid substrate, during which the density of the deposited particles is directly proportional to the duration of collection. In a previous study, we combined electrospray with masking to deposit biomacromolecular nanoparticles on uniaxially-aligned electrospun nanofibers in a linear density gradient.[29] It was shown that collagen nanoparticles in a unidirectional gradient on the uniaxially-aligned nanofibers promoted the migration of bone marrow stem cells in the direction of increasing particle density. On the uniaxially-aligned nanofibers functionalized with collagen nanoparticles in a bidirectional gradient, fibroblasts migrated from two opposite sides towards the center of the scaffold in the direction of increasing particle density. The migration speed of fibroblasts on the uniaxially-aligned nanofibers was higher in the presence of bidirectional gradient than the case involving uniform distribution of the same nanoparticles. Gradients can be readily produced in a controllable and reproducible fashion by adjusting the parameters for electrospray. This class of scaffolds shows great potential as biomedical patches for a variety of biomedical applications such as bone regeneration, wound healing, and nerve repair.

Here we demonstrate that the capability of this strategy can be extended to generate a radial density gradient of nanoparticles on a scaffold comprised of radially-aligned nanofibers. Such scaffolds could be further empowered to accelerate cell migration from the periphery towards the center for the speedy closure of a wound. As a major component of ECM, collagen is widely considered as one of the most prominent biomolecules to affect cellular behaviors. Accordingly, collagen nanoparticles can be applied as a biological effector to regulate cell adhesion, proliferation, and migration. Specifically, as shown in Figure 1, we can apply a scaffold made of radially-aligned nanofibers as the collector for electrospray while an aperture with tunable opening size is placed between the metallic needle and the collector during electrospray. The opening of the aperture can be tuned to vary the duration of collection for the nanoparticles, resulting in a decrease in particle density from the center to the periphery of the collector. As a major advantage, this simple and general method can be adapted for various types of solid substrates and electrosprayed particles. We firstly investigate the effects of a radial density gradient of collagen nanoparticles fabricated on a circular glass slide on the migration of fibroblasts from the periphery towards the center. To understand the corresponding effects of the gradient and the radially-aligned nanofibers, we further investigate the synergetic effect arising from the radial density gradient of collagen nanoparticles and the radially-aligned nanofibers on the migration of fibroblasts for the potential application in wound closure.

2. Results and Discussion

2.1. Glass slide covered by collagen nanoparticles in a radial density gradient

In our initial demonstration, we used electrospray to fabricate collagen nanoparticles in a radial density gradient on a solid substrate such as a circular glass slide. Prior to electrospray, a tunable aperture with a full opening of 36 mm in diameter was imposed between the metallic needle and the collector (Figure 1). The aperture was closed at the beginning so that the electrosprayed nanoparticles were completely blocked by the closed aperture. As the aperture was opened at a fixed speed, the size of the opening was gradually increased, through which the electrosprayed nanoparticles were deposited onto the surface of the collector. In this setting, the center of the collector should experience the longest duration of exposure to the electrosprayed nanoparticles, resulting in a gradual decrease in particle density from the center to the periphery.

In a typical procedure, we opened the aperture at a fixed speed to increase the opening size by 1.0 mm in diameter per minute and collected the nanoparticles for 15 min to generate a radial density gradient of collagen nanoparticles on the surface of a circular glass slide. Figure S1 shows scanning electron microscopy (SEM) images of the nanoparticles electrosprayed onto different regions on the glass slide, corresponding to different durations of collection. From the center to the periphery region, the area densities of the nanoparticles on the glass slide gradually decreased as the duration of collection decreased from 15 to 10 and 5 minutes. The collagen nanoparticles had a more or less hemispherical shape, together with an average diameter of 370 ± 125 nm at their base in contact with the substrate (Figure S2).

In order to visualize and quantify the radial gradient by fluorescence microscopy imaging, we encapsulated rhodamine-B in the collagen nanoparticles during electrospray. Figure 2, A–D, shows fluorescence micrographs of the nanoparticles deposited at different positions on the glass slide. Along the radial direction from the center to the periphery, the nanoparticles were gradually reduced in density, indicating the successful generation of a radial density gradient. In Figure 2E, we plotted the relative fluorescence intensities as a function of distance from the center to the periphery of the glass slide along the radial direction. Away from the center, the relative fluorescence intensity decreased as a function of the distance, with a difference of almost seven times. In principle, rhodamine-B can also be replaced by other types of bioactive proteins or growth factors as long as their bioactivities can be preserved during the electrospray process to endow the nanoparticles with additional bioactivity. In addition, other types of ECM components, such as laminin and fibronectin, can be mixed with collagen prior to electrospray to further enhance the functionality of the nanoparticles.

The profile of the radial density gradient can be readily maneuvered by adjusting the size of the substrate, the deposition rate of the particles, the total duration of collection, and/or the opening speed of the aperture. To demonstrate the versatility of this method, we fabricated another radial density gradient of collagen nanoparticles on a circular glass slide of 25 mm in diameter. In this case, the aperture was opened at a fixed speed to increase the opening size by 1.0 mm in diameter per minute, and the nanoparticles were collected on the glass

slide for a total duration of 30 minutes. Figure S3 shows the relative fluorescence intensity of rhodamine B-loaded collagen nanoparticles as a function of distance from the center to the periphery of the glass slide, indicating the creation of a radial gradient in particle density (n = 3).

2.2. Cell migration on glass slide covered by radially-graded collagen nanoparticles

Centripetal migration of cells from the surroundings towards the center is beneficial to a variety of applications, such as to speed up wound closure and promote the regeneration of dura mater, as well as to the repair of retinal nerve. The migration speed of the cells can be accelerated because of their haptotaxis through the attractive cues immobilized on the surface of a substrate. Here we examined the influence of the radial density gradient of collagen nanoparticles on the centripetal migration of cells using NIH 3T3 fibroblasts as a model. In a typical experiment, a piece of circular glass slide functionalized with radially-graded collagen nanoparticles was fixed to the bottom of a well in a 24-well plate. We also included glass slides without collagen nanoparticles and covered by a uniform distribution of collagen nanoparticles as the control groups. A polydimethylsiloxane (PDMS) cylinder with a diameter of 6.0 mm was placed in the center of the sample as a physical barrier to create a “wound”. Then, NIH-3T3 fibroblasts were seeded around the periphery of the cylinder. After 4 h, the cylinder was removed to create a migration zone. Figure 3A shows fluorescence micrographs of NIH-3T3 fibroblasts after migration for three days on different types of substrates, respectively. On the substrate functionalized with radially-graded collagen nanoparticles (graded), the cells reached the center of the substrate, and a large number of cells were observed in the central region. By contrast, fewer cells were found in the migration zone of the glass slide functionalized with uniformly-distributed collagen nanoparticles (uniform). In particular, very few cells appeared in the central region of the bare glass slide (blank). From the fluorescence micrographs of cells in the leading regions of the migration zones, the cells on the different types of substrates all showed healthy states with random extension of their cytoskeleton. In the frontiers of the migration zone on the graded substrate, a substantially larger number of cells were found. The radial density gradient of the collagen nanoparticles significantly promoted cell migration towards the region with an increased content of collagen along the radial direction.

We then counted the average number of cells in different regions of the migration zones on the different types of substrates from the fluorescence micrographs. As illustrated in Figure S4 and in the inset of Figure 3B, the radial migration zone with a radius of 3 mm was equally divided into eight equally-sized slices, and each slice was further divided into six concentric regions (I to VI) of equal width from the periphery to the center at an incremental distance of 0.5 mm. Figure 3B shows the average numbers of cells in the different regions of the migration zone on the different types of substrates. In the outer region of the migration zone (region I), the cell number was too high to be precisely counted, so we only showed the average numbers of cells in the other five regions (II-VI). On the graded substrate, the cells in the leading region could migrate to the central region VI and distributed throughout the six regions of the whole migration zone, whereas much fewer cells could migrate to the central region VI on the uniform substrate. In each region of the migration zone, significantly more cells were presented on the graded substrate in comparison to that on the

uniform substrate ($P < 0.01$). On the bare glass slide, the cells were only able to migrate to region II. Taken together, it can be concluded that considerably more cells were able to migrate to the central region on the graded substrate, relative to both the glass slide covered with a uniform coating of collagen nanoparticles ($P < 0.01$) and the bare glass slide ($P < 0.01$).

The farthest migration distances of collective cells on the different types of substrates are shown in Figure 3C. On the glass slide functionalized with radially-graded collagen nanoparticles, the migration distance of the collective cells was increased by 3.2- and 2.1-fold, respectively, relative to those on the glass slides without collagen nanoparticles and functionalized with uniformly-distributed collagen nanoparticles. Cells tend to migrate faster on the substrates functionalized with graded collagen nanoparticles than those with a uniform distribution of the nanoparticles, mainly because of the haptotactic cue provided by the collagen gradient, which could promote cells to migrate towards a higher particle density and thus a higher collagen content. Taken together, these results indicate that masked electrospray technique can be used to fabricate a radial density gradient of collagen nanoparticles on a solid substrate to promote cell migration towards the region with the greatest particle density.

2.3. Radially-aligned nanofibers functionalized with collagen nanoparticles in a radial density gradient

In addition to the use of flat substrates such as glass slides, this masked electrospray technique has also been successfully applied to generate radial density gradients of collagen nanoparticles on other types of substrates. In one demonstration, the collagen nanoparticles were directly electrosprayed on a scaffold of radially-aligned nanofibers because the nanofibers can provide the topographic cue to guide cell migration along the radial direction. We firstly fabricated the scaffold composed of radially-aligned electrospun polycaprolactone (PCL) nanofibers using a collector consisting of a metallic ring and a metallic needle in the center. The electrospun nanofibers were stretched across the gap between the needle and the ring in a radially-aligned fashion. As shown by the SEM images in Figure S5, the PCL nanofibers were radially aligned from the center towards the periphery of the scaffold, together with an average fiber diameter of 608 ± 132 nm.

Figure 4 shows SEM images of the radially-aligned PCL nanofibers at different distances from the center, after functionalization with electrosprayed collagen nanoparticles marked by a false color. The original SEM images can be found in Figure S6. The as-deposited nanoparticles were more or less fused together with the surfaces of the nanofibers without involving additional treatment because of electrostatic attraction and the presence of some residual solvent in the particles during electrospray. After solidification, the particles would not move and aggregate because they stuck to the surfaces of the nanofibers. In addition, the collagen nanoparticles were insoluble in water or cell culture medium. Taken together, the nanoparticles were largely retained during the seeding of cells and even after three days of cell migration study. In the central region (Figure 4A), the surface of the nanofibers was covered by a high density of collagen nanoparticles, as marked by the color dots. As the collection time decreased from the center to the periphery, fewer collagen nanoparticles

would be deposited on the surface of the nanofibers. In the peripheral region corresponding to 6-mm away from the center, the surface of the nanofibers had a very low density of collagen nanoparticles (Figure 4D). Taken together, we can directly electrospray collagen nanoparticles onto a scaffold of radially-aligned nanofibers to create a radial density gradient, with the density decreasing from the center to the periphery along the radial direction of the scaffold.

2.4. Cell migration on the radially-aligned nanofibers functionalized with radially-graded collagen nanoparticles

Scaffolds comprised of radially-aligned nanofibers can promote wound closure by promoting cell migration along the radial direction. To investigate the combined effect of radial alignment and particle density gradient on the migration of NIH-3T3 fibroblasts, we fabricated a scaffold (diameter: 12 mm) of radially-aligned nanofibers functionalized with collagen nanoparticles in a radial density gradient decreasing from the center to the periphery. For comparison, we also fabricated scaffolds of radially-aligned nanofibers without collagen nanoparticles and functionalized with uniformly-distributed collagen nanoparticles. A similar protocol involving the use of a PDMS cylinder was applied to study cell migration on the different types of scaffolds from the periphery towards the center. We fixed and stained the cells to reveal their positions on the different types of scaffolds, as shown by the fluorescence micrographs in Figure 5A. On the fiber-based scaffolds, all the cells were stretched and migrated along the direction of fiber alignment, indicating the contact guidance from the underneath nanofibers to the cells. Compared with the bare nanofibers, the presence of the collagen nanoparticles, regardless of the distribution pattern, significantly increased the number of cells in the migration zone because of the bioactivity of the collagen component. Furthermore, the cells migrated faster on the scaffold functionalized with radially-graded collagen nanoparticles than that with a uniform distribution of collagen nanoparticles because of the haptotactic cue provided by the collagen gradient, which tended to promote cells to migrate towards a higher content of collagen. On the graded scaffold, the cells almost covered the entire area of the migration zone, and a large number of cells were observed in the center. In comparison, fewer cells were observed in the migration zone of the uniform scaffold.

Figure 5, B and C, shows the areas of the voids left behind by the cells and the farthest migration distance of the collective cells on the different types of scaffolds, respectively. The percentage of void left by the cells in the central region of the graded scaffold was less than 2%, while that number on the uniform scaffold and the bare nanofibers increased to about 7% and 25%, respectively, indicating that the “wound” closure was significantly promoted by combining the radially-aligned nanofibers and the radial density gradient. The migration distance of the collective cells on the graded scaffold was increased by 1.6- and 1.3-fold, respectively, relative to those on the scaffolds functionalized with uniformly-distributed collagen nanoparticles and involving no collagen nanoparticles ($P < 0.01$). In addition, the migration of cells on the substrates involving radially-aligned nanofibers was significantly promoted relative to the case of glass slides.

The morphologies of the cells in the central and peripheral regions of the different types of scaffolds can be seen from the fluorescence micrographs in Figure 6. The cytoskeleton took an elongated morphology and large extension on the radially-aligned nanofibers. In addition, more cells were presented in the central region of the graded scaffold in comparison with that on the uniform scaffold. Almost no cells were able to migrate to the central region of the scaffold comprised of bare nanofibers. From these results, we can conclude that the particle density gradient and the fiber alignment had a synergetic effect in promoting the centripetal migration of cells towards the region with the greatest particle density. Both the topographic cue of the scaffold arising from the radially-aligned nanofibers and the haptotactic cue enabled by the graded nanoparticles contribute to the acceleration of cell migration from the periphery towards the center, showing great promise for future application in tissue regeneration.

2.6. Discussion

A radial density gradient of collagen nanoparticles can be created on a scaffold of radially-aligned nanofibers by masked electrospray with a tunable aperture mask. As a result, cell migration can be maximized by a unique combination of the topographic cue arising from the radially-aligned nanofibers and a haptotactic cue enabled by the graded nanoparticles. Under the guidance of the radially-aligned nanofibers, the cells polarize and move forward along the fiber alignment. In response to the gradient of collagen nanoparticles that can serve as an adhesive cue, the cells are further guided to migrate according to the direction of pre-established polarity. The response of cells to the scaffold may depend on cell-cell adhesions and microtubules,[30,31] and cadherin mechanotransduction can also play a potential role.[32] In order to provide a haptotactic cue capable of guiding the directional migration of cells, the slope of the gradient should be greater than a certain value. As such, the diameter of the scaffold cannot be increased indefinitely. However, at a fixed slope, the area to be covered by the gradient of particles can be enlarged by increasing the number of particles deposited at the center. To this end, a new aperture will be necessary, and the collection time will also need to be optimized.

The variation in particle density gradient can also affect the migration of cells. In general, haptotaxis directs cells to move along a gradient of increasing density in the immobilized ligand. However, the cell movement distance and speed may vary when the slope of the particle density gradient is changed. At the same time, the surface roughness of the as-obtained fibers will be changed with the deposition of nanoparticles, and this will introduce another factor that can influence the cell behavior. Therefore, the mechanism responsible for the migration of cells on the particle-coated nanofibers can be a complicated one, which deserves a systematic study in the future. The slope of the gradient also needs to be optimized in the future to maximize the efficacy of such a scaffold in promoting cell migration.

As a major advantage, this method can be readily applied to many other types of fiber scaffolds, including those consisting of aligned or random fibers made of different types of polymers because the deposition method depends on neither the orientation of the fibers nor the type of the polymer. In addition to collagen, this method can be applied to other types of

biomacromolecules in ECM, such as laminin and fibronectin, to target different applications. If necessary, the collagen nanoparticles can also be loaded with drugs or growth factors *via* co-axial electrospray to endow the scaffolds with a variety of biochemical cues to improve the functionality. To maximize the efficacy of such a scaffold in accelerating cell migration for promoting the reconstruction of new tissue and improving the wound healing, the size and shape of the nanoparticles, as well as the profile of the gradient will need to be optimized systematically. In the future, we plan to demonstrate the capability of this new class of scaffolds for promoting *in vivo* skin wound healing by inducing the migration of repairable cells from the periphery towards the center of the defect site.

This new class of scaffolds can also be applied to treat glaucoma and other retinal degenerative diseases by mimicking the radial orientation of the axons in the retina. In a prior study, radially-aligned electrospun fibers were used to direct the radial growth of retinal ganglion cell axons and enhanced the retinal ganglion cell survival.[33] When the fibers loaded with the cells were transplanted onto retinal explants, the cells on the scaffold followed the radial pattern of the host retinal nerve fibers. To this end, the scaffold of radially-aligned nanofibers can serve as a cell delivery device, representing a significant step forward towards the use of cell transplant therapies for the treatment of glaucoma and other retinal degenerative diseases. When further integrated with the radial density gradient of biomacromolecular nanoparticles, the neurite extension should be further promoted.

Radial alignment, together with a radial gradient, is important for a variety of biological processes and technical applications. In addition to tissue regeneration, the surface comprised of radial alignment and radial gradient may also show promise in other applications, such as directional liquid transportation[26] and directional guidance of DNA[34] because of the accompanied wettability gradient along the particle density gradient. Many natural surfaces have directional liquid wetting and transportation properties to allow cactuses and spider silk to collect fresh water from fog by transporting droplets from the periphery to the center.[35] Different from surface engineering based on asymmetric chemical modification or geometrical patterning, the masked electrospray technique, in combination with electrospun fibers, does not require complex procedures while allowing for facial tuning of the gradient in terms of slope, as well as size and composition of the particles.

3. Conclusion

In summary, using masked electrospray with a tunable aperture, we have demonstrated the generation of a radial density gradient of collagen nanoparticles on both a flat substrate and a scaffold comprised of radially-aligned nanofibers, respectively, with the particle density decreasing from the center to the periphery. The radial density gradient of collagen nanoparticles on the glass slide promoted the centripetal migration of NIH-3T3 cells from the periphery along the direction of increasing particle density. When the collagen nanoparticles were deposited on a scaffold made of radially-aligned nanofibers in a radially-graded fashion, the cell migration on the scaffold was significantly accelerated in comparison with the case of a uniform distribution. The acceleration could be attributed to the unique combination of the topographic cue arising from the radially-aligned nanofibers

and the haptotactic cue enabled by the graded collagen nanoparticles. This study provides valuable information for designing graded scaffolds integrated with a radially-aligned topographic cue for potential use in wound closure and related applications that require cell migration in a radial pattern.

4. Experimental Section

Chemicals and materials:

PCL (M_w≈80,000), *N,N*-dimethylformamide, dichloromethane, and Type IV collagen were purchased from Sigma-Aldrich. All other chemicals were obtained from Thermo Fisher Scientific. The water used in all experiments was obtained by filtering through a set of Millipore cartridges (Epure, Dubuque, IA). An aperture with a diameter of 36 mm was purchased from Thorlabs™.

Generation and characterization of a radial density gradient of collagen nanoparticles on a glass slide:

We masked electrospray with a tunable aperture to generate a radial density gradient of collagen nanoparticles on a glass slide. In a typical process, collagen was dissolved in 70% aqueous acetic acid (v/v) to prepare a collagen solution at a concentration of 20 mg/mL. A circular glass slide (*ca.* 12 mm in diameter) was cleaned with ethanol, treated with plasma, and then placed on top of an aluminum foil to serve as the collector. A tunable aperture was placed between the needle and the collector. The collagen solution was then pumped out through a blunt needle at a feeding rate of 0.5 mL/h while a high voltage (DC) of 20 kV was applied between the tip of the needle and the collector. During the electrospray process, the aperture was opened at a fixed speed to generate openings with gradually increased sizes, allowing more nanoparticles electrosprayed onto the glass slide. In a typical experiment, the aperture was opened at a fixed speed to increase the opening size by 1.0 mm in diameter per minute, and the nanoparticles were deposited on the glass slide over a duration of 15 min.

The morphologies of the nanoparticles deposited at different positions on the glass slide were characterized using a scanning electron microscope (Hitachi SU8230). The average diameter of the nanoparticles was measured from 100 nanoparticles in the SEM images using ImageJ software (NIH, Bethesda, MD, USA).

Visualization of the radial density gradient of collagen nanoparticles on a glass slide:

A collagen solution containing 5 mg/mL of rhodamine-B was electrosprayed through the aperture mask to fabricate a radial density gradient of collagen nanoparticles loaded with rhodamine-B. The as-obtained samples were analyzed using an inverted fluorescence microscope (Leica DMI 6000 B). From the center to the periphery, four images were recorded from different positions with the same incremental distance along the radial axis. The average fluorescence intensity at each position was measured using ImageJ software, and the relative fluorescence intensities were plotted as a function of distance away from the center of the circular glass slide. In another set of experiment, circular glass slides with a diameter of 25 mm were used as the collectors. During the electrospray process, the aperture was opened at a fixed speed to increase the opening size by 1.0 mm in diameter per minute,

and the nanoparticles were deposited on the glass slides over a duration of 30 min. The as-obtained samples were also analyzed using the fluorescence microscope, and the relative fluorescence intensities were measured at different positions.

Migration of NIH-3T3 fibroblasts on the glass slides:

We investigated the migration of NIH-3T3 fibroblasts on the glass slides with a diameter of 12 mm after functionalization with radially-graded collagen nanoparticles, together with bare glass slides and slides covered with uniformly-distributed collagen nanoparticles as control groups. The glass slide covered by collagen nanoparticles in a uniform distribution was fabricated by directly electrospraying the particles onto the glass slide. The total number of collagen nanoparticles deposited on the surface was almost the same when comparing masked electrospray for 15 min with the case of direct electrospray for 7 min. In a typical masked electrospray process, the aperture was opened at a speed to increase the opening size by 1.0 mm in diameter per minute, and the nanoparticles were deposited on the glass slide (diameter =12 mm) over a duration of 15 min. In this case, assuming that the number of nanoparticles deposited on per unit area of the glass slide per unit time during electrospray was n and the electrospray time was t, the total number of deposited collagen nanoparticles was: $N = \int_0^{12} \pi\left(\frac{t}{2}\right)^2 ndt + (15-12)\pi r^2 n = 252\pi n$. When the electrospray process was performed without the use of the mask, the nanoparticles were directly deposited onto the whole surface of the glass slide with a diameter of 12 mm. After deposition for 7 min, the total number of deposited collagen nanoparticles could be calculated as: $N = 7\pi r^2 n = 7\pi 6^2 n = 252\pi n$. Since the flow rate of the electrospray solution was set as the same, the total number of collagen nanoparticles deposited on the surface should be more or less the same when comparing masked electrospray for 15 min with the case of direct electrospray for 7 min. To demonstrate the advantage of the graded pattern, we slightly prolonged the duration of collection to 7.5 min for direct electrospray to cover the glass slide with uniformly-distributed collagen nanoparticles.

The samples were affixed to the bottom of the wells in a 24-well plate. Triplicate samples in each group were used for the study. In each well, a PDMS cylinder with a diameter of 6 mm was placed in the center of the sample as a physical block to generate a wound, and NIH-3T3 fibroblasts cultured in Dulbecco's modified eagle medium supplemented with 10% fetal bovine serum and 1% antibiotic-antimycotic were seeded at a concentration of 1×10^5 cells/mL around the periphery of the cylinder. After 4 h, the cylinders were removed to allow the cells to migrate inward. After incubation for another three days, the cells were fixed in 3% glutaraldehyde solution at room temperature for 10 min and permeabilized with 0.1% Triton X-100 for 5 min. Afterwards, the cells were stained with Alexa Fluor 555 phalloidin and 4′,6-diamidino-2-phenylindole (DAPI), respectively. Between each procedure, the samples were washed three times with phosphate buffered saline (PBS) solution. After staining, the cells were imaged under a laser confocal scanning microscope (Zeiss 700) using a tile mode. Micrographs were taken at both low and high magnifications to analyze the distribution and morphologies of cells, respectively, on the different types of samples. From the fluorescence micrographs, the migration distances of cells on the different samples were measured. The migration zone on each sample was

divided into six regions with the same incremental distance along the radial axis from the center to the periphery. The numbers of cells within different regions in the migration zone were counted from the fluorescence micrographs of DAPI staining using ImageJ software. Triplicate samples in each group were used for the study.

Fabrication and characterization of radially-aligned PCL nanofibers:

A scaffold made of radially-aligned electrospun PCL nanofibers was fabricated using a metallic ring (*ca.* 15 mm in diameter) as the collector, together with a sharp needle in the center. Briefly, PCL pellets were dissolved in a mixture of dichloromethane and *N,N*-dimethylformamide at a volume ratio of 80:20 to prepare a PCL solution at a concentration of 10 wt.%. Afterwards, the solution was fed through a blunt needle at a rate of 1.0 mL/h, and a high voltage (DC) of 15 kV was applied between the tip of the needle and the grounded collector. After electrospinning for 30 min, the high voltage was terminated. The radially-aligned nanofibers were transferred onto a circular glass slide of 12 mm in diameter and affixed with a medical silicone adhesive. The fibers deposited on the glass slide were characterized using a scanning electron microscope (SU8230). The average diameter of the fibers was measured from 100 fibers in the SEM images using ImageJ software.

Generation and characterization of a radial density gradient of collagen nanoparticles on a scaffold of radially-aligned PCL nanofibers:

We utilized the same method discussed above to generate a radial density gradient of collagen nanoparticles on a scaffold of radially-aligned PCL nanofibers. The scaffold was affixed to a circular glass slide of 12 mm in diameter and used as the collector. During the electrospray process, the aperture was opened at a fixed speed to increase the opening size by 1.0 mm in diameter per minute, and the nanoparticles were deposited on the nanofibers over a duration of 15 min. Scaffolds consisting of radially-aligned nanofibers covered by collagen nanoparticles in a uniform distribution were fabricated by directly electrospraying the nanoparticles onto the nanofibers over a duration of 7.5 min. SEM was used to characterize the morphology of the radially-aligned nanofibers functionalized with the nanoparticles in a radial density gradient.

Migration of NIH-3T3 fibroblasts on the scaffolds of radially-aligned nanofibers:

We investigated the migration of NIH-3T3 fibroblasts on the radially-aligned nanofibers functionalized with collagen nanoparticles in a radial density gradient using the same method as described above. Bare nanofibers and nanofibers covered with collagen nanoparticles in a uniform distribution served as the control groups. The samples were affixed to the bottom of the wells in a 24-well plate. Triplicate samples in each group were used for the study. After incubation for another three days, the cells were fixed and stained with Alexa Fluor 555 phalloidin and DAPI, respectively, and then imaged under the laser confocal scanning microscope using a tile mode. From the fluorescence micrographs, the percentages of the voids left behind by the NIH-3T3 cells and the farthest migration distance of collective cells on the different types of scaffolds were analyzed from the fluorescence micrographs using ImageJ software.

Statistical Analysis:

All the values were averaged at least in triplicate and presented in the form of mean ± standard deviation, with "n" indicating the number of samples per group. Comparison between groups was performed using one-way ANOVA, followed by Student's t-tests for all pairwise comparisons. Differences were considered statistically significant when $P < 0.05$.

Supplementary Material

Refer to Web version on PubMed Central for supplementary material.

Acknowledgements

This work was supported in part by a grant from the National Institutes of Health (R01 EB020050) and startup funds from the Georgia Institute of Technology.

References

[1]. Weijer CJ, J. Cell Sci 2009, 122, 3215. [PubMed: 19726631]
[2]. Trepat X, Chen Z, Jacobson K, Compr. Physiol 2012, 2, 2369. [PubMed: 23720251]
[3]. Qu F, Guilak F, Mauck RL, Nat. Rev. Rheumatol 2019, 15, 167. [PubMed: 30617265]
[4]. Friedl P, Gilmour D, Nat. Rev. Mol. Cell Biol 2009, 10, 445. [PubMed: 19546857]
[5]. Li L, He Y, Zhao M, Jiang J, Burns Trauma 2013, 1, 21. [PubMed: 27574618]
[6]. Tahara N, Brush M, Kawakami Y, Dev. Dyn 2016, 245, 774. [PubMed: 27085002]
[7]. Xiao Y, Riahi R, Torab P, Zhang DD, Wong PK, ACS Nano 2019, 13, 1204. [PubMed: 30758172]
[8]. Zheng W, Yuan X, Cell Adh. Migr 2008, 2, 48. [PubMed: 19262126]
[9]. Kim JI, Kim JY, Park CH, Sci. Rep 2018, 8, 3424. [PubMed: 29467436]
[10]. Chen S, Wang H, Su Y, John JV, McCarthy A, Wong SL, Xie J, Acta Biomater 2020, 108, 153. [PubMed: 32268240]
[11]. Xie J, Macewan MR, Ray WZ, Liu W, Siewe DY, Xia Y, ACS Nano 2010, 4, 5027. [PubMed: 20695478]
[12]. Chen G, Sima J, Jin M, Wang KY, Xue XJ, Zheng W, Ding YQ, Yuan XB, Nat. Neurosci 2008, 11, 36. [PubMed: 18059265]
[13]. Li X, Li M, Sun J, Zhuang Y, Shi J, Guan D, Chen Y, Dai J, Small 2016, 12, 5009. [PubMed: 27442189]
[14]. Aragona M, Dekoninck S, Rulands S, Lenglez S, Mascré G, Simons BD, Blanpain C, Nat. Commun 2017, 8, 14684. [PubMed: 28248284]
[15]. Song KH, Heo S-J, Peredo AP, Davidson MD, Mauck RL, Burdick JA, Adv. Healthc. Mater 2020, 9, e1901228. [PubMed: 31867881]
[16]. Xue J, Xie J, Liu W, Xia Y, Acc. Chem. Res 2017, 50, 1976. [PubMed: 28777535]
[17]. Xue J, Wu T, Dai Y, Xia Y, Chem. Rev 2019, 119, 5298. [PubMed: 30916938]
[18]. Xue J, Pisignano D, Xia Y, Adv. Sci 2020, 7, 2000735.
[19]. Dong Y, Zheng Y, Zhang K, Yao Y, Wang L, Li X, Yu J, Ding B, Adv. Fiber Mater 2020, 2, 212.
[20]. Kador KE, Montero RB, Venugopalan P, Hertz J, Zindell AN, Valenzuela DA, Uddin MS, Lavik EB, Muller KJ, Andreopoulos FM, Goldberg JL, Biomaterials 2013, 34, 4242. [PubMed: 23489919]
[21]. Kador KE, Grogan SP, Dorthé EW, Venugopalan P, Malek MF, Goldberg JL, D'Lima DD, Tissue Eng. Part A 2016, 22, 286. [PubMed: 26729061]
[22]. Shaker MR, Lee JH, Park SH, Kim JY, Son GH, Son JW, Park BH, Rhyu IJ, Kim H, Sun W, Stem Cell Rep 2020, 15, 898.
[23]. Yang D, Zhao Z, Bai F, Wang S, Tomsia AP, Bai H, Adv. Healthc. Mater 2017, 6, 201700472.

[24]. Chen S, McCarthy A, John JV, Su Y, Xie J, Adv. Mater 2020, 32, e2003754. [PubMed: 32944991]

[25]. Zhu C, Qiu J, Thomopoulos S, Xia Y, Adv. Healthc. Mater 2021, 10, e2002269. [PubMed: 33694312]

[26]. Li J, Qin QH, Shah A, Ras RHA, Tian X, Jokinen V, Sci. Adv 2016, 2, e1600148. [PubMed: 27386574]

[27]. Collinson MM, Higgins DA, Langmuir 2017, 33, 13719. [PubMed: 28849936]

[28]. Wu T, Xue J, Li H, Zhu C, Mo X, Xia Y, ACS Appl. Mater. Interfaces 2018, 10, 8536. [PubMed: 29420008]

[29]. Xue J, Wu T, Qiu J, Rutledge S, Tanes ML, Xia Y, Adv. Funct. Mater 2020, 30, 202002031.

[30]. Etienne-Manneville S, Subcell Biochem 2012, 60, 225. [PubMed: 22674074]

[31]. Costa P, Blowes LM, Laly AC, Connelly JT, Acta Biomater 2021, 126, 291. [PubMed: 33741539]

[32]. Khalil AA, de Rooij J, Exp. Cell Res 2019, 376, 86. [PubMed: 30633881]

[33]. Kador KE, Montero RB, Venugopalan P, Hertz J, Zindell AN, Valenzuela DA, Uddin MS, Lavik EB, Muller KJ, Andreopoulos FM, Goldberg JL, Biomaterials 2013, 34, 4242. [PubMed: 23489919]

[34]. Giri D, Li Z, Ashraf KM, Collinson MM, Higgins DA, ACS Appl. Mater. Interfaces 2016, 8, 24265. [PubMed: 27541167]

[35]. Zheng Y, Bai H, Huang Z, Tian X, Nie FQ, Zhao Y, Zhai J, Jiang L, Nature 2010, 463, 640. [PubMed: 20130646]

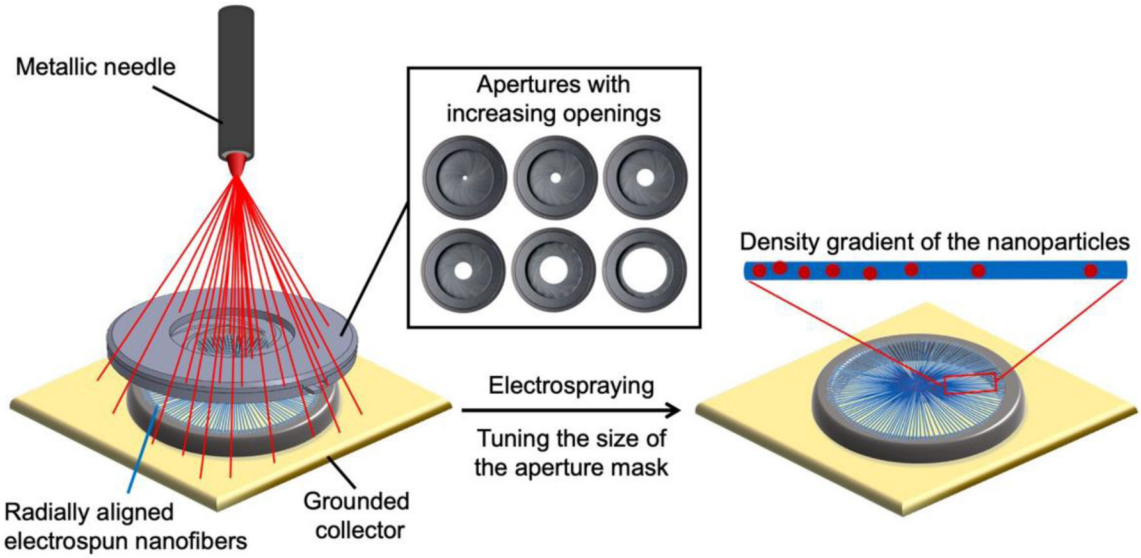

Figure 1.

A schematic of how to fabricate collagen nanoparticles in a radial density gradient on the surface of radially-aligned nanofibers. A size-tunable aperture is imposed as a mask between the needle and the grounded collector. During the electrospray process, the aperture is gradually opened to shorten the duration of nanoparticle collection from the center to the periphery.

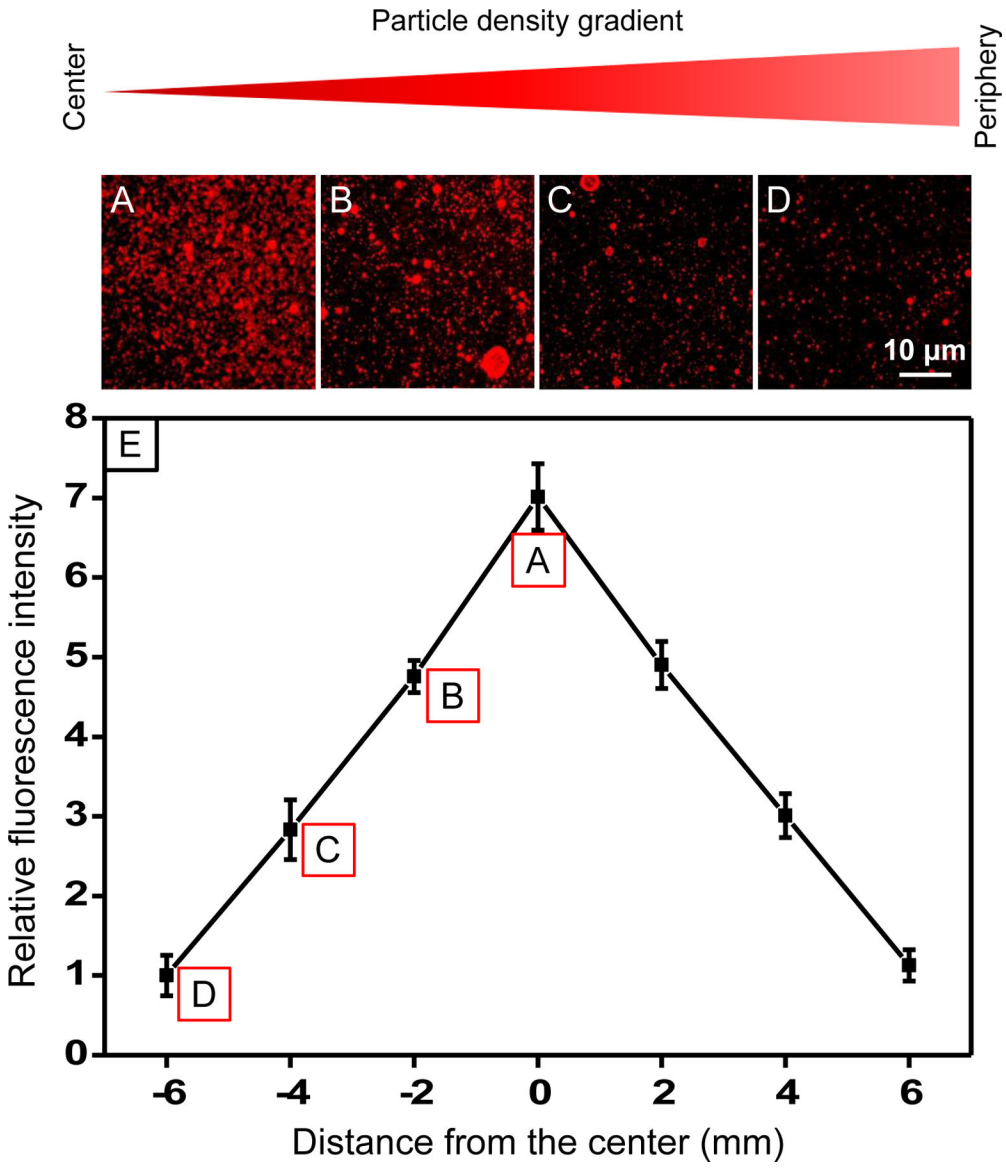

Figure 2.

(A–D) Representative fluorescence micrographs and (E) the relative fluorescence intensity of rhodamine B-loaded collagen nanoparticles as a function of distance from the center to the periphery of a circular glass slide with a diameter of 12 mm, indicating the formation of a radial gradient in particle density that decreases from the center to the periphery (n = 3). The aperture was opened at a fixed speed to increase the opening size by 1.0 mm in diameter per minute. The nanoparticles were deposited on the glass slide at a total collection duration of 15 min. The difference of the gradient from the central to the peripheral region can be controlled by adjusting the size of the substrate, the deposition rate of the electrosprayed particles, the duration of electrospray, and/or the opening speed of the aperture.

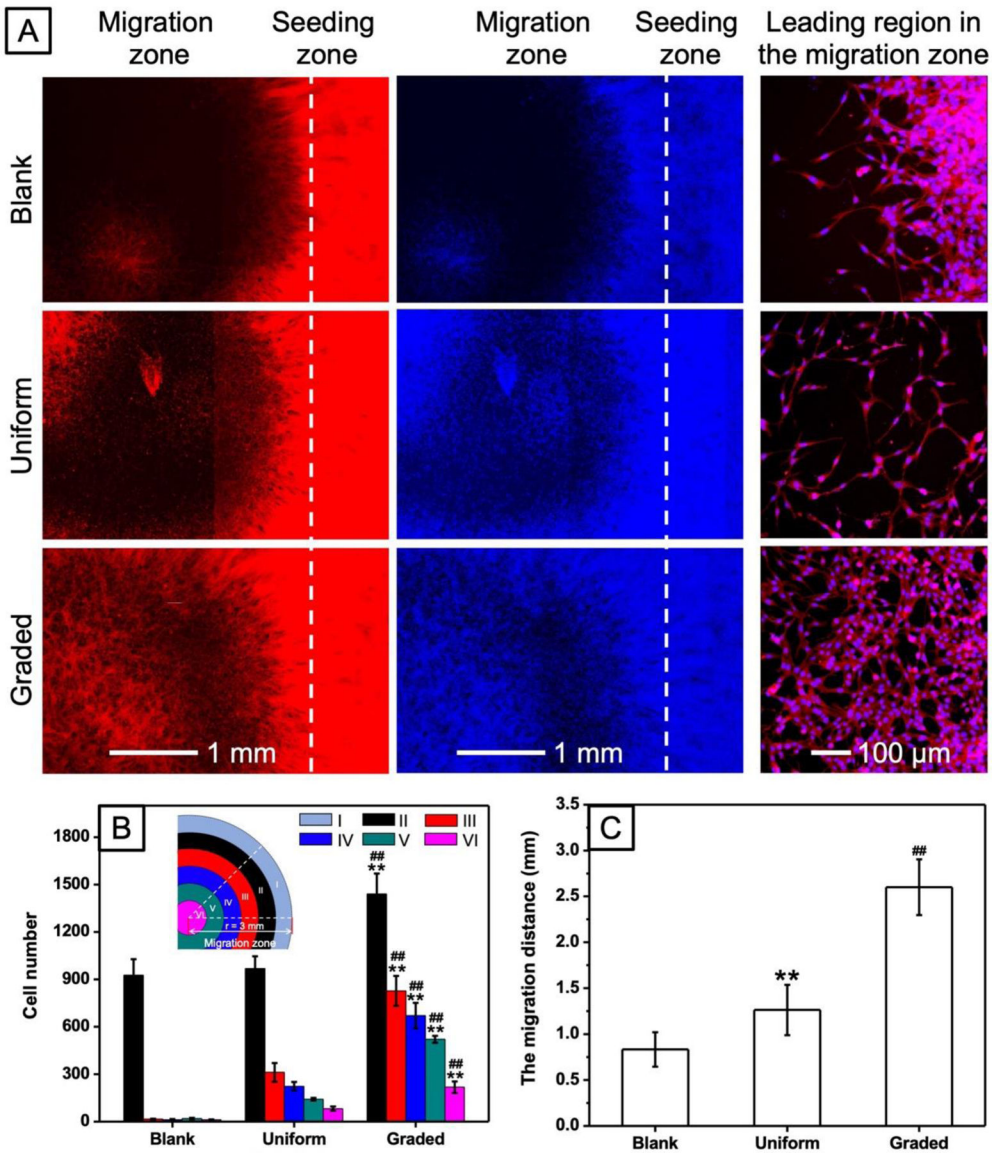

Figure 3.

(A) Fluorescence micrographs showing the migration of NIH-3T3 cells from the periphery to the center and the morphology of cells in the leading region of the migration zone on glass slides without collagen nanoparticles (blank), with uniformly-distributed collagen nanoparticles (uniform), and with radially-graded collagen nanoparticles (graded), respectively. F-actin and nuclei of the cells were stained with Alexa Fluor 555-phollodin (red) and DAPI (blue), respectively, to help visualize the migration behavior of cells on the different types of substrates. (B) The number of NIH-3T3 cells in different regions (regions II–VI, as indicated by the schematic in the inset) of the migration zones on the different types of substrates, respectively. $^{**}P < 0.01$ when comparing the graded group with the blank group (n = 3). $^{\#\#}P < 0.01$ when comparing the graded group with the uniform group (n = 3). (C) The migration distance of cells on the different types of substrates. $^{**}P <$

0.01 when comparing the uniform group with the blank group (n = 3). $^{\#\#}P < 0.01$ when comparing the graded group with the blank group (n = 3).

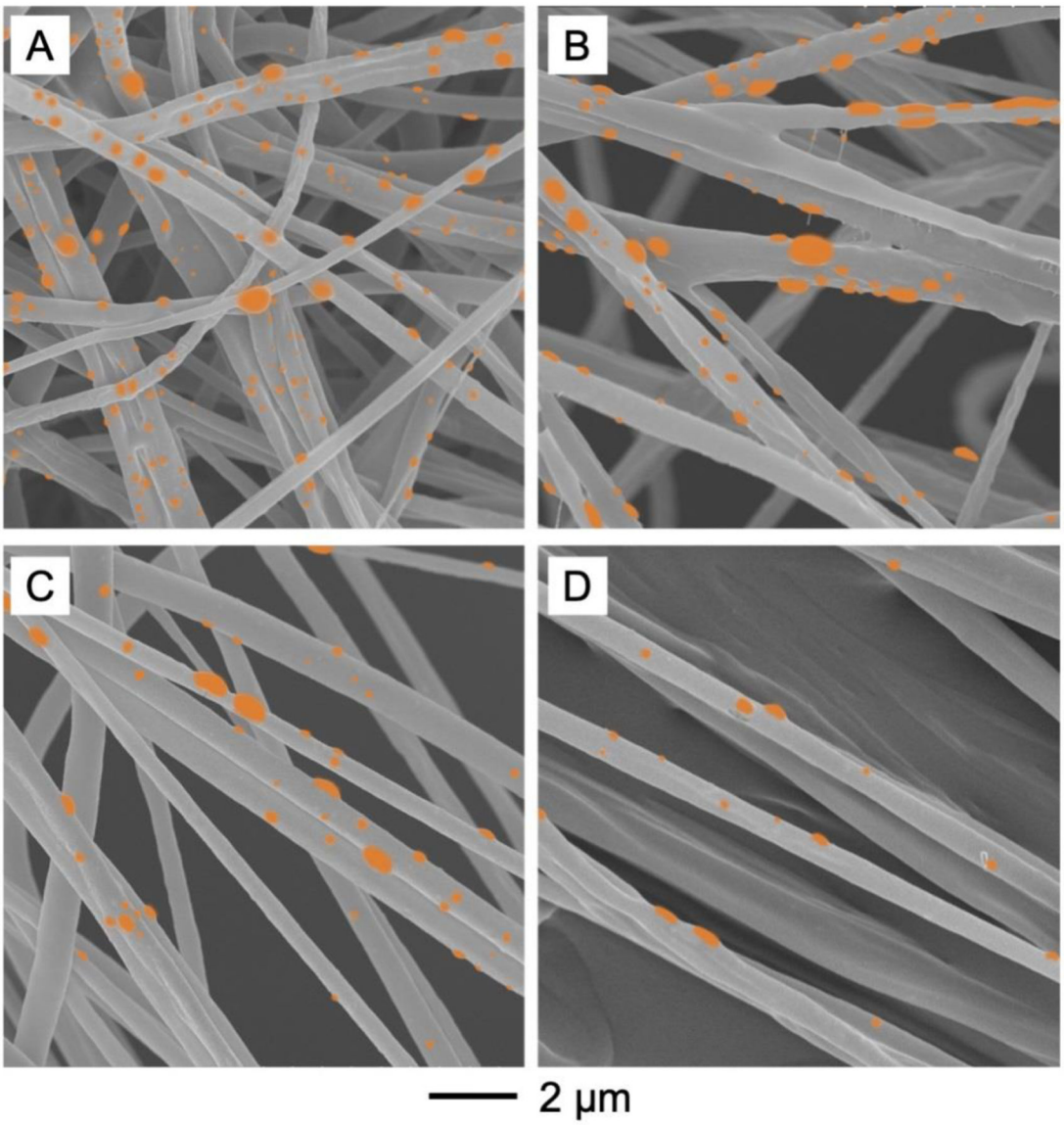

Figure 4.

SEM images of radially-aligned PCL nanofibers functionalized with electrosprayed collagen nanoparticles at different distances from the center: (A) 0, (B) 2, (C) 4, (D) 6 mm, respectively. The density of the electrosprayed nanoparticles decreased from the center to the periphery along the radially-aligned nanofibers, indicating a radial gradient in terms of particle density. The color dots correspond to the collagen nanoparticles.

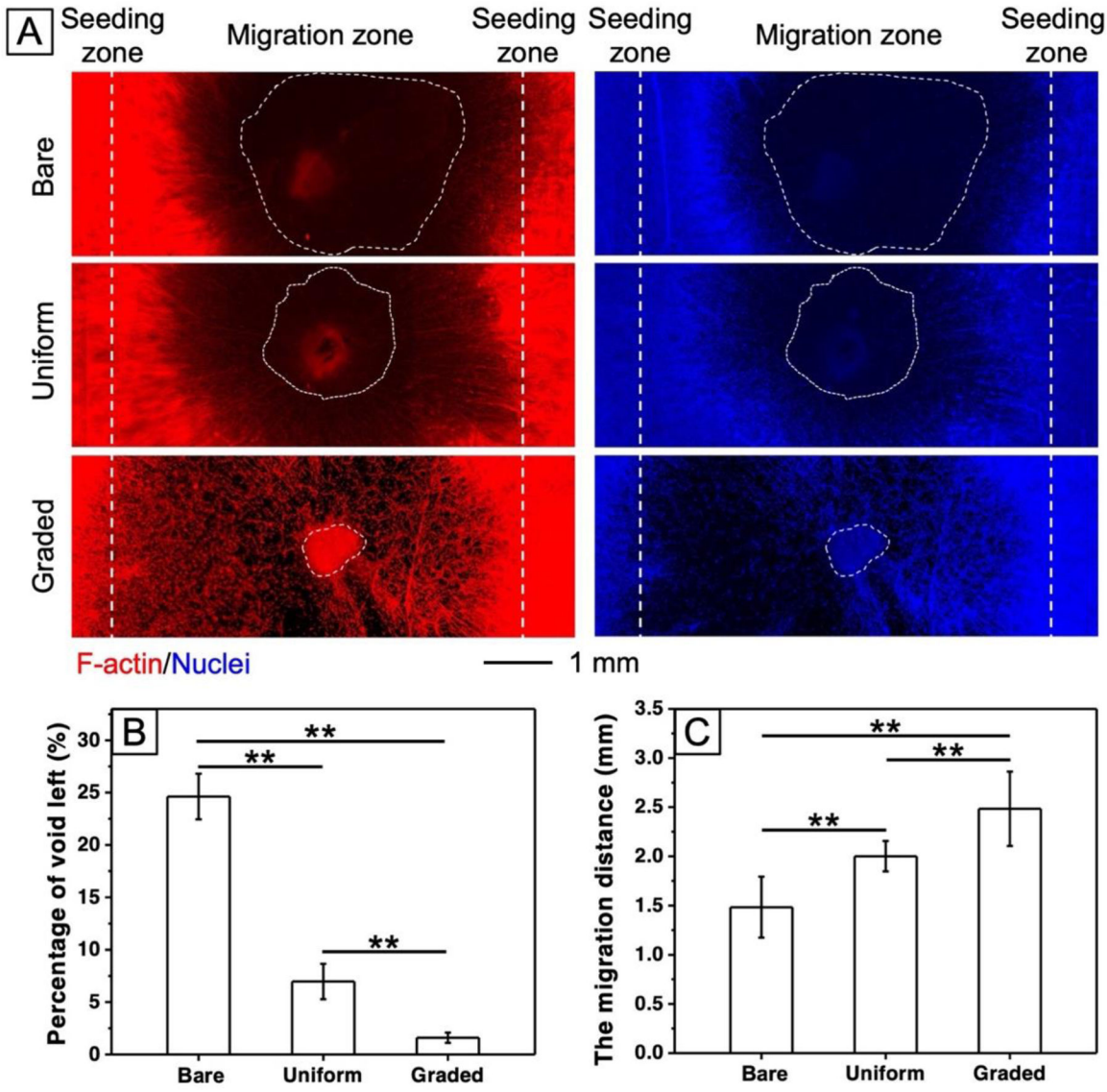

Figure 5.

Fluorescence micrographs showing the migration of NIH-3T3 cells from the periphery to the center on the surface of radially-aligned nanofibers before (bare) and after functionalized with uniformly-distributed (uniform) or radially-graded collagen nanoparticles (graded). The void was defined as the region not covered by cells in the central region. F-actin and nuclei of the cells were stained with Alexa Fluor 555-phollodin (red) and DAPI (blue), respectively, to help analyze the migration behavior of cells on the different types of substrates. (B) Percentage of the void left behind by the NIH-3T3 cells on the different types of substrates. $^{**}P < 0.01$ (n = 3). (C) The farthest migration distance of cells on the different types of substrates. $^{**}P < 0.01$ (n = 3).

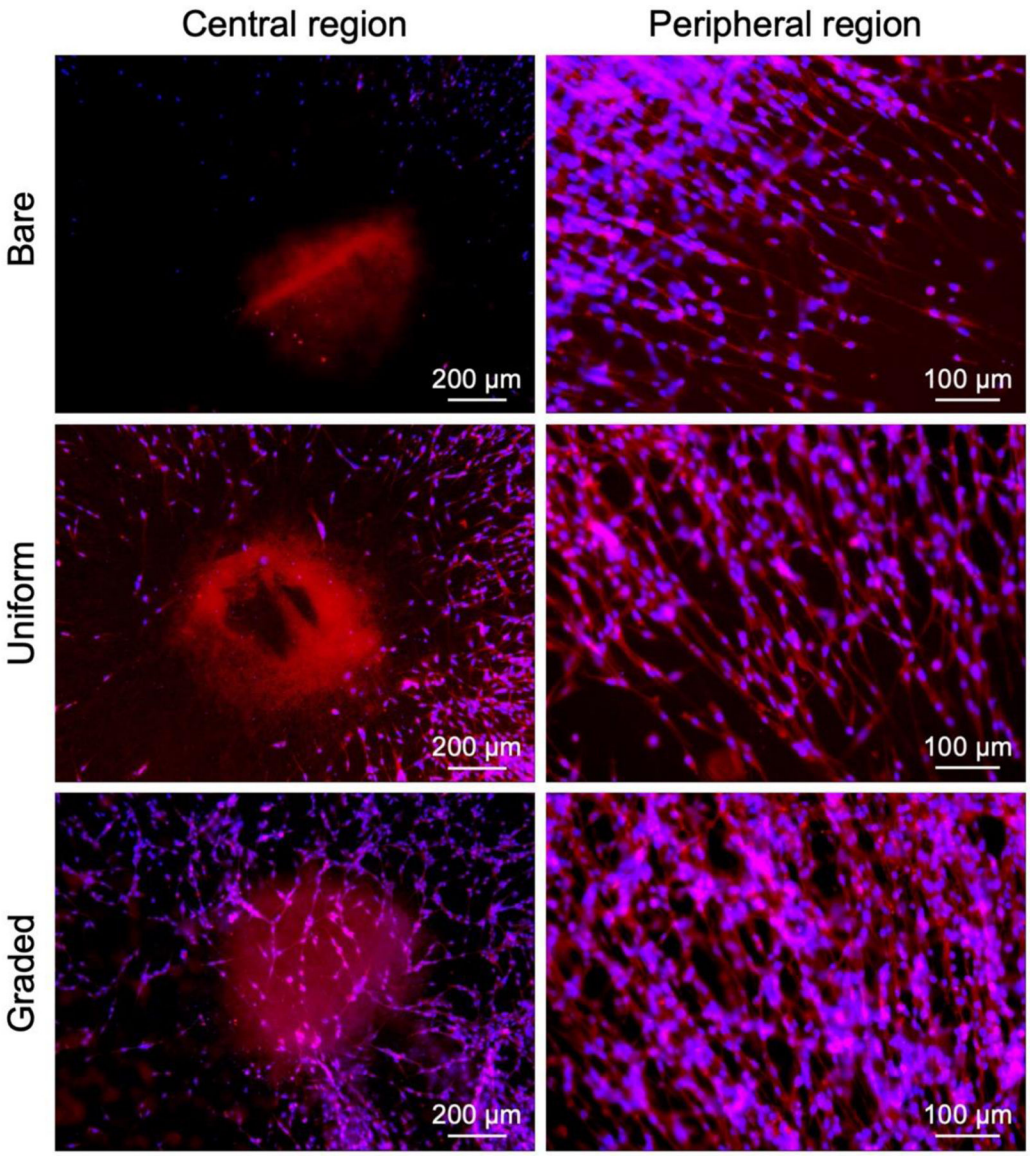

Figure 6.

Fluorescence micrographs showing the morphology of NIH-3T3 cells at the central and peripheral regions after migration for three days on the surface of radially-aligned nanofibers before (bare) and after functionalized with uniformly-distributed collagen nanoparticles (uniform) and radially-graded collagen nanoparticles (graded), respectively. F-actin and nuclei of the cells were stained with Alexa Fluor 555-phollodin (red) and DAPI (blue), respectively.